第32卷第7期 中国有色金属学报 2022年 7月
Volume 32 Number 7 The Chinese Journal of Nonferrous Metals July 2022
DOI: 10.11817/j.ysxb.1004.0609. 2021-41081

Ni-Mn-Ga合金马氏体相变温度与相变温度跨度的等静压调控

胡粉娥[1]，魏生贤[2,3]，季鹏成[2]，刘兆轩[2]，陈 源[2]，杨林碹[2]，何禧佳[2,3]，陶 昌[2]

(1. 曲靖师范学院 化学与环境科学学院，曲靖 655011；
2. 曲靖师范学院 物理与电子工程学院，曲靖 655011；
3. 曲靖师范学院 磁性材料及器件研究中心，曲靖 655011)

摘 要：Ni-Mn基合金在磁驱动器、传感器、固态磁制冷、负热膨胀材料等领域具有潜在的应用价值。相变温度跨度较窄制约了Ni-Mn基合金的实际应用。为了有效拓宽相变温度跨度，以$Ni_{55.5}Mn_{18}Ga_{26.5}$为研究对象，利用实验手段研究合金的结构、相变特性以及相变温度跨度与等静压的内在关系。结果表明：合金在室温下为四方马氏体结构，其马氏体相变温度高于室温。马氏体相变温度与相变温度跨度均随等静压的增大而逐步增大。在正、反马氏体相变过程中，相变峰值温度与相变温度跨度对等静压的敏感度分别约为29.35、25.88 K/GPa和42.11、39.46 K/GPa。显然，等静压的应用不仅有利于驱动Ni-Mn-Ga合金的马氏体相变，而且有助于其相变温度跨度的拓宽。这些研究结果为Ni-Mn-Ga合金相变的调控与相变温度跨度的拓宽具有较好的指导意义。

关键词：Ni-Mn-Ga合金；马氏体相变；等静压；相变温度；相变温度跨度

文章编号：1004-0609(2022)-07-1975-08 **中图分类号**：O469 **文献标志码**：A

引文格式：胡粉娥, 魏生贤, 季鹏成, 等. Ni-Mn-Ga合金马氏体相变温度与相变温度跨度的等静压调控[J]. 中国有色金属学报, 2022, 32(7): 1975−1982. DOI: 10.11817/j.ysxb.1004.0609. 2021-41081

HU Fen-e, WEI Sheng-xian, JI Peng-cheng, et al. Hydrostatic controlling of martensitic transformation temperature and transformation temperature span of Ni-Mn-Ga alloys[J]. The Chinese Journal of Nonferrous Metals, 2022, 32(7): 1975−1982. DOI: 10.11817/j.ysxb.1004.0609. 2021-41081

Ni-Mn基合金是一类重要的多功能材料，在马氏体相变过程中展现出丰富的物理效应，如形状记忆效应[1]、磁电阻效应[2−3]、磁热效应[2−5]、压热效应[5−6]、负热膨胀效应[7−8]等。由于这些效应在工程技术方面的潜在应用而备受关注。研究表明，上述效应的大小与一级结构相变(马氏体相变)和二级磁转变(居里转变)密切相关[3−6]。当一级相变与二级相变同时发生，构成磁−结构相变时，上述物理效应会显著增强[2−8]。但近年来的研究显示，马氏体相变温度跨度(ΔT)较窄是制约Ni-Mn基合金走向实际应用的主要因素之一[9−10]。值得注意的是，$BaTiO_3$[11]、Pr-Ga化合物[12]、Mn_3-Ge-N化合物[13−14]、Fe-Mn-Ga合金[15]等材料的应用也存在同样的瓶颈问题。因此，寻求较宽温度范围内具有磁−

基金项目：国家自然科学基金资助项目(12064035，51861032，51862032)；云南省地方本科高校联合专项−面上项目(2017FH001-047，2017FH001-054)；国家级大学生创新创业训练计划项目(201910684007)；省级大学生创新创业训练计划项目(202010684031)；云南省高校科技创新团队支持计划

收稿日期：2021-06-09；**修订日期**：2021-09-23

通信作者：魏生贤，教授，博士；电话：0874-8987852；E-mail：wsx_8600@163.com

结构相变的材料是科学和技术应用上的一个挑战。从当前的研究进展来看，增大相变温度跨度的主要方法有：1) 组分调节[16−17]；2) 元素掺杂[18−20]；3) 适当的热处理[21−22]；4) 将工作温区不同的物质混合[23−24]；5) 利用多物理场，如磁场、单轴应力、等静压激发相变[5, 25−26]等。前三种方法简单、对ΔT的拓宽较为有限；第四种方法工艺相对复杂，但ΔT的拓宽较为显著。Ni-Mn-Ga合金的相变温度对磁场敏感度较低，约为1 K/T；对等静压的敏感度相对较高、在6~20 K/GPa，甚至更高。例如，对于$Ni_{53}Mn_{21}Ga_{26}$合金，施加0~0.54 GPa等静压可使其ΔT从10 K提高至20 K，ΔT对等静压的敏感度约为18.7~22.7 K/GPa[27]。这说明利用等静压对ΔT进行调控是科学可行的。为了拓宽Ni-Mn基合金的相变温度跨度，本文以磁−结构相变合金$Ni_{55.5}Mn_{18}Ga_{26.5}$为研究对象，研究了等静压对其马氏体相变温度及相变温度跨度的影响。测量过程中，磁场H_o=0.05 T，等静压p为0~0.80 GPa(样品未被施加等静压时，p=0 GPa)。结果显示，随着等静压的增大，相变温度逐步增大。相变峰值温度(T_M)对等静压的响应dT_M/dp约为29.35 K/GPa，与利用克劳修斯−克拉珀龙方程计算结果基本一致。正、反马氏体相变温度跨度对p的敏感度分别为42.11、39.46 K/GPa。这些结果显示，相变温度及相变温度跨度对等静压的敏感度较高。因此，等静压的应用对$Ni_{55.5}Mn_{18}Ga_{26.5}$合金马氏体相变的驱动与相变温度跨度的拓展具有较强的促进作用。研究结果可为Ni-Mn基体系合金马氏体相变温度及相变温度跨度的调控具有较好的指导意义。

1 实验

将纯度高于99.98%的镍(Ni)、锰(Mn)、镓(Ga)金属单质按名义组分$Ni_{55.5}Mn_{18}Ga_{26.5}$配好后，在高纯氩气保护下利用真空电弧炉反复熔炼4次，以制备实验所需合金样品。为避免合金样品组分偏析，熔炼过程中辅以磁力搅拌。将制备好的合金锭置于高纯氩气保护的石英管中，1073 K条件下持续退火72 h，然后快速投入冰水混合物中进行淬火处理。利用DK7720电火花数控线切割机将样品切成条状或块状，选取中间部分用于样品的性能测试。样品的实际组分由PW-100-017型扫描电子显微镜(Scanning electron microscope，SEM，Netherlands)附带的能量色散光谱仪(Energy-dispersive spectrometer，EDS)进行测定。测定结果显示，样品的实际组分为$Ni_{55.62}Mn_{17.52}Ga_{26.86}$，实际组分与名义组分的相对误差≤2.74%，两者基本一致。样品室温下的晶体结构由Ultima-IV型多功能X射线衍射仪(X-ray diffractometer，XRD，Japan)加以表征。马氏体相变温度由TA Instruments DSC 2000型差示扫描热分析仪(Differential scanning calorimetry，DSC，America)加以测定，测试速率为10 K/min。利用物性测量系统(Physical properties measurement system，PPMS，America)振动样品磁强计(Vibrating sample magnetometer，VSM)测量样品磁化强度(Magnetization，H)随温度(T)变化的热磁曲线$H(T)$，以便确定样品在外加磁场(H_o)与外加等静压(p)下的马氏体相变温度，升降温测试速率为1.5 K/min。零场下的热应变曲线采用标准应变仪接入PPMS系统进行测试，测试速率为3 K/min。利用VSM附带的铜−铍夹型压力包进行样品等静压作用下的磁测量。测试时，将质量约为8 mg的样品装入特氟龙胶囊中，灌入矿物油(Daphne 7373)作为压力传导介质，然后将胶囊置于铜−铍夹型压力包内进行加压测试，升降温速率为1 K/min。

2 结果与分析

2.1 合金粉末X射线衍射分析

图1所示为$Ni_{55.5}Mn_{18}Ga_{26.5}$合金室温下粉末的XRD谱及其Rietveld精修结果，其中I_{calc}与I_{obs}分别表示衍射强度的Rietveld精修计算值与实验观测值，$I_{obs}-I_{calc}$表示两者的绝对误差。由图1可知，Rietveld精修值与实验观测值吻合较好，且每一个米勒指数(Miller index)都与四方非调制马氏体结构一一对应[16, 27]。由此可知，合金在室温下为马氏体结构，其马氏体相变温度高于室温。精修结果显示，马氏体相的晶格参数为a=b=0.38761 nm、c=0.64682 nm；合金的体密度ρ=8298 kg/m^3，与$Ni_{53}Mn_{21}Ga_{26}$(8250 kg/m^3)[27]、$Ni_{55}Mn_{20}Ga_{25}$(8285 kg/m^3)[28]的密度相近。由晶格参数可计算出合金在马氏体相的摩尔体积V_M=7.313 cm^3/mol，与$Ni_{58.3}Mn_{17.1}Ga_{24.6}$(7.21 cm^3/mol)[29]、$Ni_{53}Mn_{21}Ga_{26}$

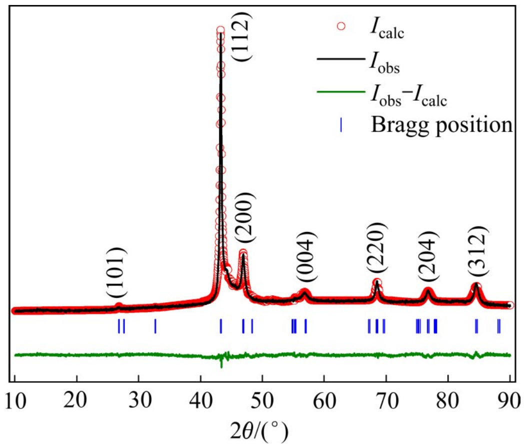

图1　室温下$Ni_{55.5}Mn_{18}Ga_{26.5}$合金粉末的XRD谱

Fig. 1　XRD patterns for $Ni_{55.5}Mn_{18}Ga_{26.5}$ alloy powder at room temperature

(7.36 cm^3/mol)[27]合金的摩尔体积相近。

2.2　大气压下合金的相变特性

为了方便表述，样品未被施加等静压时，记p=0 GPa，此时样品处于环境大气压下。当p=0 GPa时，实验测得合金样品的DSC曲线与$H(T)$曲线分别如图2与3所示。图中，M_s与M_f分别代表正马氏体相变的开始温度与结束温度，而A_s与A_f则表示反马氏体相变的开始温度与结束温度。上述相变温度可由双切线法[30−32]加以确定，如图2与3所示；降温与升温过程的相变峰值温度由$T_M=(M_s+M_f)/2$、$T_A=(A_s+A_f)/2$加以估算。

由图2可知，在降温与升温过程中，DSC曲线出现了明显的放热峰与吸热峰，且吸热峰与放热峰

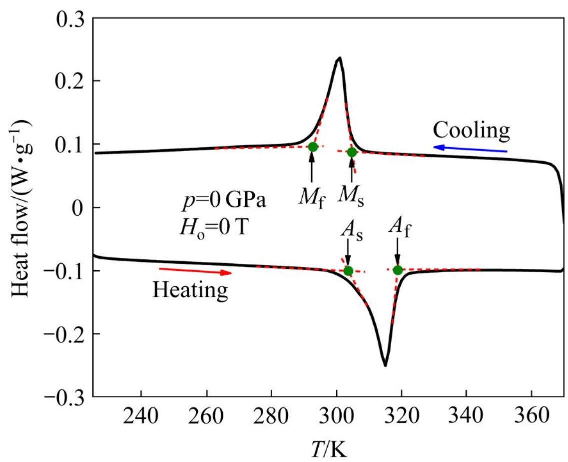

图2　$Ni_{55.5}Mn_{18}Ga_{26.5}$合金的DSC曲线

Fig. 2　DSC curves of $Ni_{55.5}Mn_{18}Ga_{26.5}$ alloy

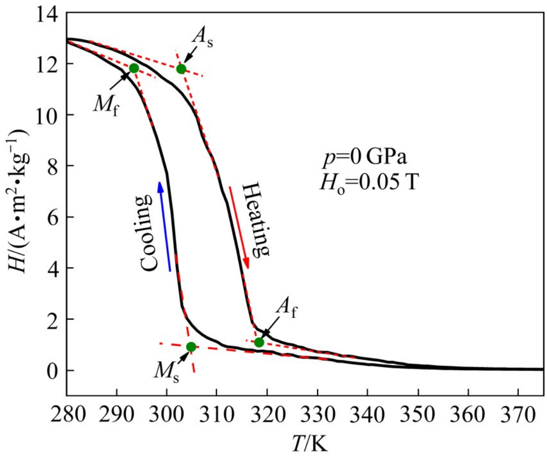

图3　$Ni_{55.5}Mn_{18}Ga_{26.5}$合金的热磁曲线$H(T)$

Fig. 3　Thermomagnetic curves $H(T)$ of $Ni_{55.5}Mn_{18}Ga_{26.5}$ alloy

存在明显的热滞后，这是一级马氏体相变的基本特征。即在降温与升温过程中，合金发生了正、反马氏体相变。相变温度M_s=304.6 K、M_f=292.6K、A_s=303.2 K、A_f=318.5K、T_M=298.6 K、T_A=310.9 K。相变温度高于室温(约293 K)，与前述XRD定性分析结果一致。

合金在马氏体相变过程中总的转变熵变可由下式计算[5]:

$$\Delta S_{tr}=\int_{M_s}^{M_f}\frac{1}{T}\left(\frac{dQ}{dt}\right)\left(\frac{dT}{dt}\right)^{-1}dT \tag{1}$$

式中：dQ/dt、dT/dt分别表示热流功率与升降温速率。利用式(1)与图2中的热流数据，可计算得出ΔS_{tr}=−20.03 J/(kg·K)(折合−1.22 J/(mol·K))。

图3所示为合金样品在低磁场(0.05 T)下、p=0 GPa时的热磁曲线$H(T)$。由图3可知，降温过程中，合金由顺磁态转化为铁磁态；随后升温过程中，合金又由铁磁态转化为顺磁态。即在升降温过程中，合金发生了二级居里转变，且存在明显的热滞后。由此可知，升、降温过程中，合金发生了磁−结构相变。由图3中的$H(T)$曲线可知，M_s=304.8 K、M_f=292.5 K、A_s=302.5 K、A_f=318.2 K、T_M=298.7 K、T_A=310.4 K。这些相变温度的数值与DSC确定的数值高度吻合。因此，下文中将利用$H(T)$曲线来确定不同等静压下的相变温度。

2.3　外加等静压下合金的相变特性

为了研究合金在等静压作用下的相变特性，实验测试了不同等静压(p为0、0.19、0.41、0.59、

0.80 GPa)下的热磁曲线。由于Ni-Mn-Ga合金相变温度对外加磁场的敏感度较低，故测试过程中外加磁场为定值H_o=0.05 T，其结果如图4所示。图中曲线显示，马氏体相变温度随等静压的增大而向高温方向移动。这种变化趋势可归结于压力稳定摩尔体积相对较小的马氏体相，在Ni-Mn-Sn-Si合金中也观察到了类似的行为[33]。此外，$H(T)$曲线随等静压的增大而变得越来越平滑、相变宽度越来越宽。这就意味着等静压的应用有利于马氏体相变温度跨度的拓宽，前期研究中已得到证实[26, 34]。

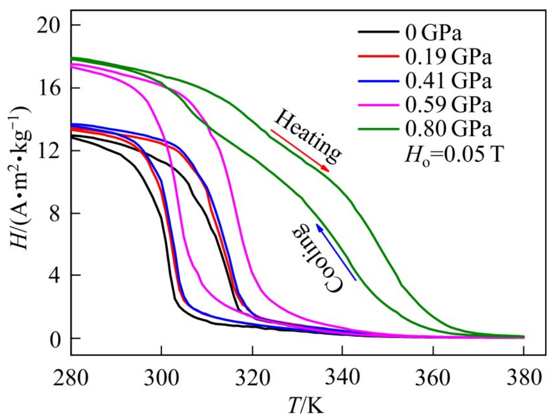

图4 不同等静压下的热磁曲线$H(T)$

Fig. 4 Thermomagnetic curves $H(T)$ at different hydrostatic pressures (Arrows along curves denote directions of increasing and decreasing temperature)

为了研究相变温度与等静压的依赖关系，课题组利用图3所示的双切线法获得了不同等静压下的马氏体相变温度。图5(a)所示为马氏体相变温度与等静压的依赖关系。由图5(a)可知：当p由0增至0.80 GPa时，M_f、A_s随等静压的增加呈线性增加；当p为0~0.60 GPa时，M_s、A_f随等静压的增加而缓慢增加；当p由0.6 GPa增至0.80 GPa时，M_s、A_f随等静压的增加而出现快速增加。线性拟合结果如表1所示。表中数据显示，在H_o=0.05 T、p为0~0.80 GPa范围内，相变温度对p的敏感度分别为dM_s/dp=50.41 K/GPa，dM_f/dp=8.30 K/GPa，dA_s/dp=6.36 K/GPa，dA_f/dp=45.40 K/GPa。

由于相变峰温$T_M=(M_s+M_f)/2$、$T_A=(A_s+A_f)/2$，而$dM_f/dp \approx dA_s/dp$，因此，T_M、T_A随等静压的增大而呈现出类似于M_s、A_f的变化趋势，如图5(b)所示。相变峰值温度T_M、T_A对p的敏感度如表1所示，且dT_M/dp=29.35K/GPa，dT_A/dp=25.88K/GPa。T_M对p的响应dT_M/dp=29.35 K/GPa，明显优于$Ni_{1.92}Mn_{1.56}Sn_{0.52}$ (18 K/GPa)[35]、$Ni_{1.9}Mn_{1.3}Ga_{0.8}$ (17 K/GPa)[36]、$Ni_{2.00}Mn_{1.32}In_{0.68}$ (18.8 K/GPa)[37]等Ni-Mn基合金；其值介于$Ni_{51.2}Mn_{31.1}Ga_{17.7}$ (25 K/GPa)[38]与$Ni_{43}Co_7Mn_{30}Ga_{20}$ (35 K/GPa)[39]之间，但与$Ni_{41.2}Co_{8.6}Mn_{32.7}Ga_{15.6}In_{1.9}$ (54 K/GPa)[40]相比还存在一定的差距，仍具有一定的优化空间。

2.4 dT_M/dp正确性的验证

dT_M/dp的正确性可由下述克劳修斯-克拉伯龙方程[40−41]加以验证：

$$\frac{dT_M}{dp}=-\frac{\varepsilon}{\rho\Delta S_{tr}} \tag{2}$$

式中：$\varepsilon=1-(1-(\Delta L/L)_{tr})^3$为相对体积变化[41]，$(\Delta L/L)_{tr}$为马氏体相变过程中合金的相变应变量，其他符号的物理含义与前面的定义一致。

合金在零场下的热应变曲线$\Delta L/L_{293}$如图7所示，下标293表示测试时的室温约为293 K。图中，点A到点B的曲线为合金样品马氏体相变对应的转变应变量，且$(\Delta L/L)_{tr}$=0.1922%，则有ε=0.568%。此数值略大于$Ni_{51.2}Mn_{31.1}Ga_{17.7}$ (ε=0.51%)[38]合金的相对体积变化。

将ΔS_{tr}=−20.03 J/(kg·K)、ρ=8298 kg/m³、ε=0.568%代入式(2)可知，dT_M/dp=34.20 K/GPa，与上述热磁曲线法测试值dT_M/dp=29.35 K/GPa基本一致。

2.5 等静压对相变温度跨度的影响

由表1数据可知，$dM_s/dp > dM_f/dp$，$dA_f/dp > dA_s/dp$。由此可预见，对于$Ni_{55.5}Mn_{18}Ga_{26.5}$合金，等

表1 相变温度、相变峰温与相变温度跨度对等静压的敏感度

Table 1 Response of transition temperatures, peak temperatures and martensitic transformation temperature spans to hydrostatic pressure

(dM_s/dp)/(K·GPa⁻¹)	(dM_f/dp)/(K·GPa⁻¹)	(dA_s/dp)/(K·GPa⁻¹)	(dA_f/dp)/(K·GPa⁻¹)	(dT_M/dp)/(K·GPa⁻¹)	(dT_A/dp)/(K·GPa⁻¹)	$(d\Delta T_d/dp)$/(K·GPa⁻¹)	$(d\Delta T_r/dp)$/(K·GPa⁻¹)
50.41	8.30	6.36	45.40	29.35	25.88	42.11	39.46

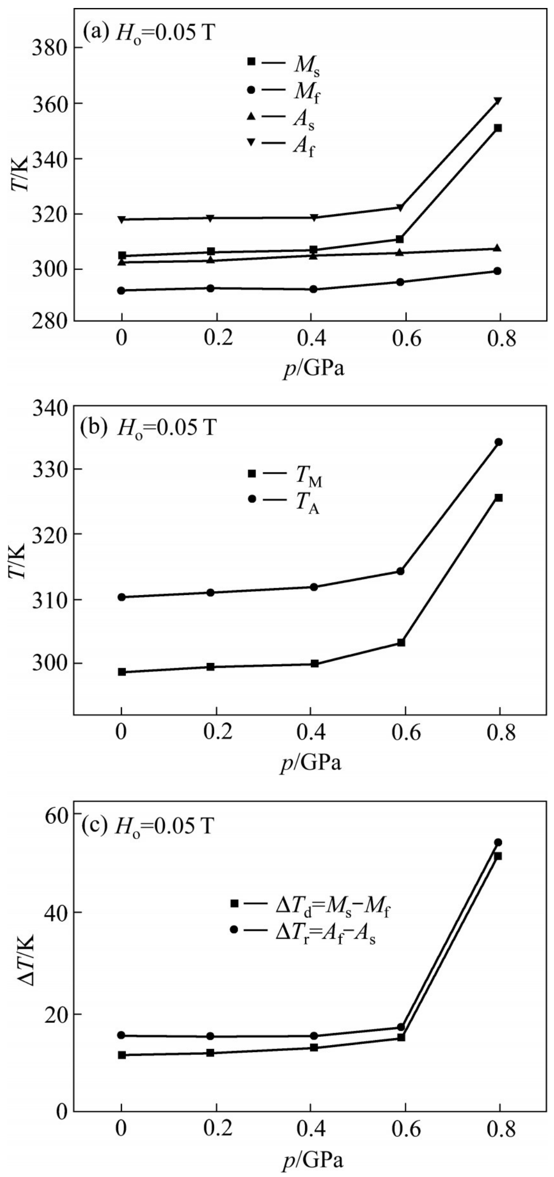

图 5　马氏体相变温度、峰温、相变温度跨度与等静压的关系

Fig. 5　Relationship between martensitic transformation temperatures(a), peak temperatures(b) and martensitic transformation temperature span(c) and hydrostatic pressure

静压的应用对其马氏体相变温度跨度的拓宽具有较大的促进作用。为了验证这一猜想，本文作者课题组对 $Ni_{55.5}Mn_{18}Ga_{26.5}$ 合金马氏体相变温度跨度 ΔT 进行了定量测试与整理，其结果如图 5(c)所示。由图 5(c)可知，$\Delta T_d=M_s-M_f$ 与 $\Delta T_r=A_f-A_s$ 分别为合金正、反马氏体相变温度的跨度。图中曲线显示，ΔT 随 p 的变化趋势与 T_M、T_A 随 p 的变化趋势相似。线性拟合结果显示，在 H_o=0.05 T、p 为 0~0.80 GPa 范围内，ΔT_d、ΔT_r 对等静压 p 的敏感度分别为 $\mathrm{d}\Delta T_d/\mathrm{d}p$=42.11 K/GPa、$\mathrm{d}\Delta T_r/\mathrm{d}p$=39.46 K/GPa。综上所述，$\Delta T$ 对 p 的敏感度较高，即等静压的应用有助于相变温度跨度的拓宽。

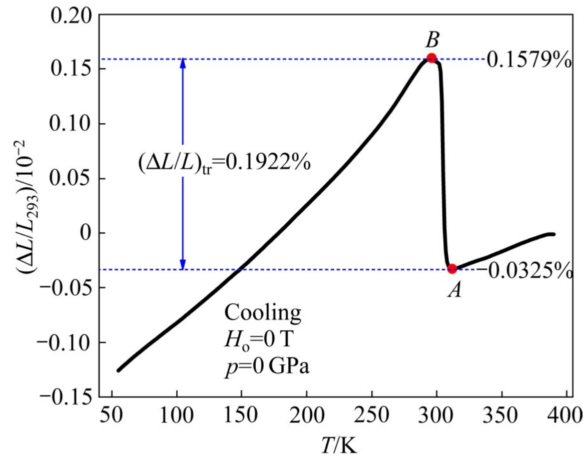

图 6　$Ni_{55.5}Mn_{18}Ga_{26.5}$ 合金降温过程的热应变曲线

Fig. 6　Thermal strain curve of $Ni_{55.5}Mn_{18}Ga_{26.5}$ alloy on cooling

3　结论

1) 粉末 XRD 谱及其 Rietveld 精修结果表明，$Ni_{55.5}Mn_{18}Ga_{26.5}$ 合金在室温下具有四方非调制马氏体结构，表明其相变温度高于室温。

2) 零场 DSC 定量分析显示，相变温度 M_s=304.6 K、M_f=292.6K、A_s=303.2 K、A_f=318.5K、T_M=298.6 K、T_A=310.9 K。相变温度高于室温(约 293 K)，与前述 XRD 定性分析结果一致。

3) 随着等静压 p 的增大，相变温度 M_s、M_f、A_s、A_f、T_M、T_A 逐步增大，对 p 的响应分别约为 50.41、8.30、6.36、45.40、29.35、25.88 K/GPa。

4) 对于所研究的合金，$\mathrm{d}T_M/\mathrm{d}p$=29.35K/GPa，与利用克劳修斯−克拉伯龙方程所计算的结果基本一致。

5) 由于相变温度对等静压的敏感度不同，即 $\mathrm{d}M_f/\mathrm{d}p\approx\mathrm{d}A_s/\mathrm{d}p$、$\mathrm{d}M_s/\mathrm{d}p>\mathrm{d}M_f/\mathrm{d}p$、$\mathrm{d}A_f/\mathrm{d}p>\mathrm{d}A_s/\mathrm{d}p$，因此，合金相变温度跨度 ΔT 对 p 的敏感度较高。正、反马氏体相变温度跨度对 p 的响应分别约为 42.11、39.46 K/GPa。由此可知，等静压的应用对 $Ni_{55.5}Mn_{18}Ga_{26.5}$ 合金马氏体相变温度跨度的拓宽具有较强的促进作用。

REFERENCES

[1] WU Y Y, WANG J M, JIANG C B, et al. Martensitic transformation, shape memory effect and mechanical properties of dual-phase $Ni_{50-x}Tb_xMn_{30}Ga_{20}$ (x=0−1) alloys[J]. Materials Science and Engineering A, 2015, 646: 288−293.

[2] PARAMANIK T, DAS I. Near room temperature giant magnetocaloric effect and giant negative magnetoresistance in Co, Ga substituted Ni-Mn-In Heusler alloy[J]. Journal of Alloys and Compounds, 2016, 654: 399−403.

[3] LUO F, HE X, RAUF S, YANG C P, et al. Influence of Al substitution on the magnetocaloric and magnetoresistance effects of $Ni_{46}Co_4Mn_{38}Sb_{12-x}Al_x$ ($0\leqslant x\leqslant 2$) alloys[J]. Journal of Magnetism and Magnetic Materials, 2020, 502: 166277.

[4] QIAN M F, ZHANG X X, LI X, et al. Magnetocaloric effect in bamboo-grained Ni-Mn-Ga microwires over a wide working temperature interval[J]. Materials & Design, 2020, 190: 108557.

[5] HU F E, WEI S X, CAO Y M, et al. Magnetocaloric and barocaloric effects associated with two successive magnetostructural transformations in $Ni_{55.5}Mn_{17.8}Ga_{26.7}$ alloy[J]. Journal of Alloys and Compounds, 2020, 818: 153356.

[6] WEI Z Y, SHEN Y, ZHANG Z, et al. Low-pressure-induced giant barocaloric effect in an all-d-metal Heusler $Ni_{35.5}Co_{14.5}Mn_{35}Ti_{15}$ magnetic shape memory alloy[J]. APL Materials, 2020, 8(5): 051101.

[7] 魏生贤, 何禧佳, 曹义明, 等. 磁制冷材料Ni-Mn-Ga合金的连续马氏体相变与奇异热膨胀特性[J]. 中国有色金属学报, 2019, 29(3): 549−558.
WEI Sheng-xian, HE Xi-jia, CAO Yi-ming, et al. Successive martensitic phase transformations and abnormal thermal expansion in Ni-MN-Ga magnetic refrigeration materials[J]. The Chinese Journal of Nonferrous Metals, 2019, 29(3): 549−558.

[8] LI Z, YANG H M, XU K, et al. Magnetocaloric and negative thermal expansion effects for $Ni_{55.5}Mn_{19.5}Ga_{25}$ Heusler alloy with magneto-structural transition[J]. Materials Chemistry and Physics, 2016, 180: 156−160.

[9] HUANG L, CONG D Y, SUO H L, et al. Giant magnetic refrigeration capacity near room temperature in $Ni_{40}Co_{10}Mn_{40}Sn_{10}$ multifunctional alloy[J]. Applied Physics Letters, 2014, 104(13): 132407.

[10] LIU J, GOTTSCHALL T, SKOKOV K P, et al. Giant magnetocaloric effect driven by structural transitions[J]. Nature Materials, 2012, 11: 620−626.

[11] LIU Y, WEI J, JANOLIN P E, et al. Giant room-temperature barocaloric effect and pressure-mediated electrocaloric effect in $BaTiO_3$ single crystal[J]. Applied Physics Letters, 2014, 104(16): 162904.

[12] HAO J Z, LIANG F X, LIU Y, et al. Hydrostatic pressure modulated spin-reorientation transition and magnetocaloric effect in PrGa compound[J]. Journal of Alloys and Compounds, 2018, 744: 426−431.

[13] TAN J, HUANG R J, LI W, et al. Broadened negative thermal expansion operation-temperature window in antiperovskite $Mn_3Zn_{0.6}Ge_{0.4}N$ prepared by spark plasma sintering[J]. Journal of Alloys and Compounds, 2014, 593: 103−105.

[14] HUANG R J, LI L F, WU Z X, et al. Spin-glass behavior in the antiperovskite manganese nitride Mn_3CuN codoped with Ge and Si[J]. Solid State Communications, 2010, 150(35/36): 1617−1620.

[15] SUN X M, CONG D Y, REN Y, et al. Giant negative thermal expansion in Fe-Mn-Ga magnetic shape memory alloys[J]. Applied Physics Letters, 2018, 113(4): 041903.

[16] PANDA A K, SINGH S, ROY R K, et al. Effect of Mn incorporation for Ni on the properties of melt spun off-stoichiometric compositions of NiMnGa alloys[J]. Journal of Magnetism and Magnetic Materials, 2011, 323(9): 1161−1169.

[17] KÖK M, AYDOĞDU Y. Effect of composition on the thermal behavior of NiMnGa alloys[J]. Journal of Thermal Analysis and Calorimetry, 2013, 113(2): 859−863.

[18] WANG J M, JIANG C B. A single-phase wide-hysteresis shape memory alloy $Ni_{50}Mn_{25}Ga_{17}Cu_8$[J]. Scripta Materialia, 2010, 62(5): 298−300.

[19] MA Y Q, YANG S Y, JIN W J, et al. $Ni_{56}Mn_{25-x}Cu_xGa_{19}$ (x= 0, 1, 2, 4, 8) high-temperature shape-memory alloys[J]. Journal of Alloys and Compounds, 2009, 471(1/2): 570−574.

[20] SÁNCHEZ-ALARCOS V, PÉREZ-LANDAZÁBAL J I, RECARTE V, et al. Correlation between composition and phase transformation temperatures in Ni-Mn-Ga-Co ferromagnetic shape memory alloys[J]. Acta Materialia, 2008, 56(19): 5370−5376.

[21] KÖK M, AYDOĞDU Y. Effect of heat treatment on the physical properties of Ni-Mn-Ga alloy[J]. Thermochimica Acta, 2012, 548: 51−55.

[22] DONG G F, GAO Z Y, SUI J H, et al. Effect of aging on phase transformation and magnetic properties of $Mn_{53}Ni_{25}Ga_{22}$ ferromagnetic shape memory alloy[J]. Journal of Magnetism and Magnetic Materials, 2015, 374: 469−473.

[23] LI L W, KADONAGA M, HUO D X, et al. Low field giant

magnetocaloric effect in *R*NiBC (*R*=Er and Gd) and enhanced refrigerant capacity in its composite materials[J]. Applied Physics Letters, 2012, 101(12): 122401.

[24] MORRISON K, BARCZA A, MOORE J D, et al. The magnetocaloric performance in pure and mixed magnetic phase CoMnSi[J]. Journal of Physics D: Applied Physics, 2010, 43(19): 195001.

[25] DE OLIVEIRA N A D. Entropy change upon magnetic field and pressure variations[J]. Applied Physics Letters, 2007, 90(5): 052501.

[26] HU F E, WEI S X, HE X J, et al. Enhanced magnetocaloric effects driven by two successive magneto-structural transformations in $Ni_{55.5}Mn_{17.8}Ga_{26.7}$ alloy under hydrostatic pressure[J]. Solid State Communications, 2019, 300: 113691.

[27] HU F E, HE X J, KANG Y R, et al. Broad operation-temperature window in $Ni_{53}Mn_{21}Ga_{26}$ alloy by applying magnetic field and hydrostatic pressure[J]. Physica B: Condensed Matter, 2021, 606: 412602.

[28] PASQUALE M, SASSO C P, LEWIS L H, et al. Magnetostructural transition and magnetocaloric effect in $Ni_{55}Mn_{20}Ga_{25}$ single crystals[J]. Physical Review B, 2005, 72(9): 094435.

[29] HE X J, XU K, WEI S X, et al. Barocaloric effect associated with magneto-structural transformation studied by an effectively indirect method for the $Ni_{58.3}Mn_{17.1}Ga_{24.6}$ Heusler alloy[J]. Journal of Materials Science, 2017, 52(5): 2915−2923.

[30] DONG G F, GAO Z Y. Effect of heat treatment on the crystal structure, martensitic transformation and magnetic properties of $Mn_{53}Ni_{25}Ga_{22}$ ferromagnetic shape memory alloy[J]. Journal of Magnetism and Magnetic Materials, 2016, 399: 185−191.

[31] KALBFLEISCH A S, MATTHEWS G, PASCAL J J. On the influence of the cooling rate on the martensitic transformation of Ni-Mn-Sn Heusler alloys[J]. Scripta Materialia, 2016, 114: 121−124.

[32] SHAMBERGER P J, OHUCHI F S. Hysteresis of the martensitic phase transition in magnetocaloric-effect Ni-Mn-Sn alloys[J]. Physical Review B, 2009, 79(14): 144407.

[33] MUTHU S E, KANAGARAJ M, SINGH S, et al. Hydrostatic pressure effects on martensitic transition, magnetic and magnetocaloric effect in Si doped Ni-Mn-Sn Heusler alloys[J]. Journal of Alloys and Compounds, 2014, 584: 175−179.

[34] 胡粉娥, 曹义明, 魏生贤, 等. Ni-Mn-Ga合金磁热效应的组分调节与等静压调控[J]. 中国有色金属学报, 2019, 29(12): 2793−2801.

HU Fen-e, CAO Yi-ming, WEI Sheng-xian, et al. Composition adjustment and hydrostatic pressure control of magnetocaloric effect in Ni-Mn-Ga alloys[J]. The Chinese Journal of Nonferrous Metals, 2019, 29(12): 2793−2801.

[35] KAŠTIL J, KAMARÁD J, ISNARD O, et al. Effect of pressure and high magnetic field on phase transitions and magnetic properties of $Ni_{1.92}Mn_{1.56}Sn_{0.52}$ and Ni_2MnSn Heusler compounds[J]. Journal of Alloys and Compounds, 2015, 650: 248−255.

[36] ALBERTINI F, KAMARÁD J, ARNOLD Z, et al. Pressure effects on the magnetocaloric properties of Ni-rich and Mn-rich Ni_2MnGa alloys[J]. Journal of Magnetism and Magnetic Materials, 2007, 316(2): 364−367.

[37] STERN-TAULATS E, PLANES A, LLOVERAS P, et al. Tailoring barocaloric and magnetocaloric properties in low-hysteresis magnetic shape memory alloys[J]. Acta Materialia, 2015, 96: 324−332.

[38] CHERNEUKO V A, KOKORIN V V, BABII O M, et al. Phase diagrams in the Ni-Mn-Ga system under compression [J]. Inlermerallics, 1998, 6(1): 29−34.

[39] KAŠTIL J, KAMARÁD J, KNÍŽEK K, et al. Peculiar magnetic properties of Er conditioned $Ni_{43}Co_7Mn_{31}Ga_{19}$ at ambient and hydrostatic pressures[J]. Journal of Alloys and Compounds, 2013, 565: 134−138.

[40] KAMARÁD J, FABBRICI S, KAŠTIL J, et al. Strong magneto-volume effects and hysteresis reduction in the In-doped $(NiCo)_2MnGa$ Heusler alloys[J]. Journal of Alloys and Compounds, 2016, 685: 142−146.

[41] HE X J, WEI S X, KANG Y R, et al. Enhanced barocaloric effect produced by hydrostatic pressure-induced martensitic transformation for $Ni_{44.6}Co_{5.5}Mn_{35.5}In_{14.4}$ Heusler alloy[J]. Scripta Materialia, 2018, 145: 58−61.

Hydrostatic controlling of martensitic transformation temperature and transformation temperature span of Ni-Mn-Ga alloys

HU Fen-e[1], WEI Sheng-xian[2, 3], JI Peng-cheng[2], LIU Zhao-xuan[2], CHEN Yuan[2],
YANG Lin-xuan[2], HE Xi-jia[2, 3], TAO Chang[2]

(1. College of Chemistry and Environmental Science, Qujing Normal University, Qujing 655011, China;
2. College of Physics and Electronic Engineering, Qujing Normal University, Qujing 655011, China;
3. Center for Magnetic Materials and Devices, Qujing Normal University, Qujing 655011, China)

Abstract: Ni-Mn based alloys have potential applications in magnetic actuators, sensors, solid state magnetic refrigeration, negative thermal expansion materials and other fields. The narrow phase transition temperature span restricts the practical application of Ni-Mn based alloys. The structure, phase transition properties and hydrostatic pressure dependence of phase transition temperature and phase transition temperature span were investigated experimentally in $Ni_{55.5}Mn_{18}Ga_{26.5}$ alloy to broaden the temperature span of phase transition. The results show that the alloy sample crystallizes in a tetragonal martensite structure at room temperature and the martensitic transformation temperatures are higher than room temperature. All the martensitic transformation temperatures and the transformation temperature span increase gradually with the increase of hydrostatic pressure. Importantly, the average sensitivity of phase transition peak temperature and phase transition temperature span to hydrostatic pressure are about 29.35, 25.88, 42.11 and 39.46 K/GPa, respectively, during the direct and reverse martensitic transformation. It is obvious that the application of hydrostatic pressure is not only beneficial to drive the martensitic transformation, but also helpful to broaden the transformation temperature span in Ni-Mn-Ga alloy. These findings are very meaningful to adjust the phase transition temperature and the broadening of phase transition temperature span in Ni-Mn-Ga alloy system.

Key words: Ni-Mn-Ga alloy; martensitic transformation; hydrostatic pressure; transformation temperature; martensitic transition temperature span

---

Foundation item: Projects(12064035, 51861032, 51862032) supported by the National Natural Science Foundation of China; Projects(2017FH001-047, 2017FH001-054) supported by the Local Colleges Applied Basic Research Projects of Yunnan Province, China; Project(201910684007) supported by the National Students' Innovation and Entrepreneurship Training Program, China; Project(202010684031) supported by the Provincial Students' Innovation and Entrepreneurship Training Program, China; Project supported by the Program for Innovative Research Team (in Science and Technology) in University of Yunnan Province, China

Received date: 2021-06-09; **Accepted date:** 2021-09-23

Corresponding author: WEI Sheng-xian; Tel: +86-874-8987852; E-mail: wsx_8600@163.com

(编辑　李艳红)